Overland JE (1984) Scale analysis of marine winds in straits and along mountainous coasts. *Monthly Weather Review* 112: 2532–2536.

Pierrehumbert RT and Wyman B (1985) Upstream effects of mesoscale mountains. *Journal of the Atmospheric Sciences* 42: 977–1003.

Stauffer DR and Warner TT (1987) A numerical study of Appalachian cold-air damming and coastal frontogenesis. *Monthly Weather Review* 115: 799–821.

Xu Q (1990) A theoretical study of cold air damming. *Journal of the Atmospheric Sciences* 47: 2969–2985.

CONTRAILS

P Minnis, NASA Langley Research Center, Hampton, VA, USA

Introduction

One of the most visible anthropogenic effects on the atmosphere is the condensation trail, or contrail. These aircraft-induced clouds have become a common sight since the 1960s because of increasing jet traffic, but they were observed as early as 1919. Contrails were frequently seen and filmed in World War II during bombing raids or dogfights. They were briefly studied in Germany during the war but drew little scientific interest again until the early 1950s when the use of jet aircraft by military and commercial aviation accelerated. Interest waned, with only sporadic studies until the 1990s when aircraft effects and contrails became the foci of numerous research efforts. Concerns over their impact on climate and aircraft visibility have been the primary motivation for the recently intensified research into contrails. Understanding their effects requires knowledge of their physical and optical characteristics and how, when, and where they form.

Contrail Formation

Contrails are generally composed of ice crystals with trace amounts of exhaust products such as soot and sulfates. The contrail ice crystals form because the relative humidity with respect to liquid water, U_w, temporarily reaches the saturation point in the plume mixture of ambient air and hot exhaust gases. Tiny droplets develop on background aerosols or on aerosols formed by exhaust compounds. Because the ambient temperatures required for formation of contrails are generally less than $-40°C$, the small water droplets instantly freeze and grow via vapor-to-ice deposition as long as the relative humidity with respect to ice, U_i, remains above the saturation point. They dissipate via sublimation if U_i is below the saturation point or by precipitation into unsaturated layers below the flight level.

Another type of contrail that forms briefly at warmer temperatures is composed of water droplets that form behind the tips or the leading edges of aircraft wings. These are commonly seen emanating from fighter aircraft in high-speed maneuvers in a humid atmosphere. In these cases, the ambient air is compressed at the wing tip and then expands quickly during adiabatic expansion within the low-pressure area above the wing tip. The expansion temporarily cools the air sufficiently that it falls below the dew point, resulting in condensation. Because ice contrails are the more common variety, the liquid water contrails are not considered further here.

The basic concepts for determining the conditions for contrail formation were developed independently by E. Schmidt in Germany during 1941 and H. Appleman in the United States during 1954. The lines in **Figure 1** schematically illustrate the ice contrail formation process for several scenarios with the ambient temperatures T_a and water vapor partial pressures e_a indicated by the points at the lower end of each line. Each line extends to the temperature T_e and water vapor partial pressure e_e of the exhaust exiting the engine. In cases defined by the lines I, II, and IV, the ambient water vapor pressure is less than the ice saturation partial pressure e_i, while in case III, $e_a > e_i$. In case I, the partial pressure exceeds e_i during the mixing but never reaches water saturation and a contrail does not develop. A short-lived contrail would develop in case II because, at point F, the mixture temperature T_F coincides with the liquid water saturation partial pressure e_w. The contrail would form when the plume temperature reached T_F and would persist until the plume partial pressure decreased to a value below e_i at approximately $-42°C$. A long-lived, persistent contrail would form in case III because the ambient air is supersaturated with respect to ice. Because saturation conditions cover a greater range of temperatures after initial formation, the contrail formed in case IV would probably last longer than that in case II.

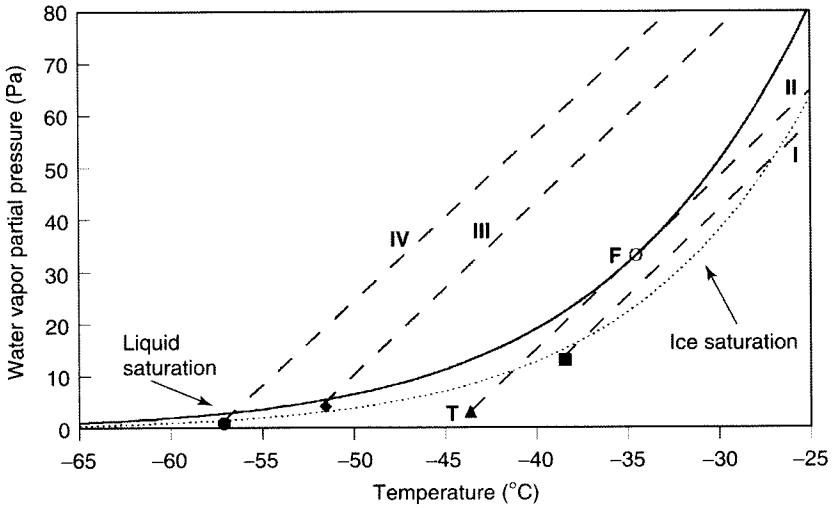

Figure 1 Phase diagram with mixing lines for aircraft exhaust in different ambient conditions.

Although contrail formation has been observed at temperatures as great as −36°C, it is clear from **Figure 1** that contrails form more easily at lower temperatures. The threshold temperature T_T for contrail formation is defined as the warmest ambient temperature that will support contrail formation for a given value of e_a and the exhaust parameters T_e and e_e. The latter quantities determine the mixing line slope, G, and are functions of engine type, operating conditions, and fuel, while the value of e_a can be determined from vertical profiles of atmospheric and dew point temperatures. In case II, the ambient temperature at point T is the contrail formation threshold temperature for the given values of e_a and the mixing line slope G. That is, the ambient temperature enabling contrail formation would have to change if either e_a or G varied and, therefore, T_T is unique for each pair of e_a and G. The threshold temperatures are greater than T_a for cases IV and III, and less than T_a for case I. To find T_T for a particular slope and e_a, it is necessary to determine the tangent point T_F for a line having slope G with the curve describing the variation of e_w with T. Given a value of G, the threshold temperature can be computed for T_F between −10°C and −60°C using eqn [1].

$$T_F = -46.46 + 9.43 \ln(G - 0.053) + 0.720 \times [\ln(G - 0.053)]^2 \quad [1]$$

where G is given in Pa K^{-1}. The threshold temperature for any value of U_w or e_a can be determined iteratively with eqn [2].

$$T_T = T_F - \frac{e_w(T_F) - U_w e_w(T_T)}{G} \quad [2]$$

The mixing line slope depends on the specific plume enthalpy h_p and the water vapor mixing ratio q, which, in turn, are related to the emission index EI_w, mass specific combustion heat Q, and the overall engine efficiency η. The relation is given specifically as eqn [3], where c_p is the specific heat capacity, p is the pressure, and $\varepsilon = 0.622$. The emission index, the mass of water produced per mass of combusted fuel, accounts for Δq since $e_e \gg e_a$.

$$G = \frac{\Delta e}{\Delta T} = \frac{(\Delta q/\Delta h_p) p c_p}{\varepsilon} = \frac{EI_w p c_p}{\varepsilon Q(1-\eta)} \quad [3]$$

The enthalpy differential is also determined almost entirely by Q and η because the ambient heat is negligible compared to that produced by the engine. Since Q and EI_w can be determined for a given fuel, the overall efficiency, the ratio of propulsion energy to total combustion energy is the primary variable affecting the mixing line slope. The slope of the line increases with increasing efficiency. Each type of engine has a nominal efficiency that is based on stationary operating conditions. The overall efficiency, however, may vary for a given engine because of different airframes, maintenance, and operating conditions. **Figure 2** illustrates the impact of efficiency for a given set of ambient conditions. In this instance η_2 is slightly less than η_1, resulting in a contrail from the plane with η_1 and no contrail from the one with η_2. Thus, two planes flying in the same environment can produce two different results. Similarly, a plane might produce a contrail when it is cruising but not when it is ascending, depending on the effect of acceleration on the efficiency.

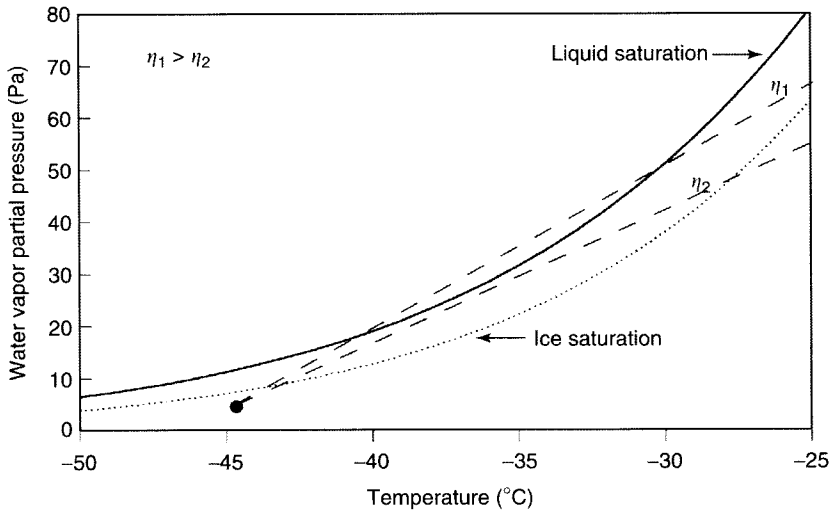

Figure 2 Hypothetical mixing lines for different propulsion efficiencies.

Contrails typically form at a distance of about 30 m or less behind the aircraft engines where the turbulent mixing sufficiently reduces the temperature. The latest research results indicate that the initial condensation of the supercooled droplets takes place on a wide variety of particles, including exhaust products such as sulfate aerosols, soot, and metallic particles as well as ambient mineral aerosols. When the contrails are about 1 minute old, the mean particle radius is around 2 μm. A wide variety of particle shapes have been observed in young contrails, including hexagonal columns and plates, triangles, irregular forms, and spheroids. Young contrails often appear saw-toothed or appear to have a cellular structure that results from the vortices formed by the aircraft. This structure provides irregularities for formation of local convective cells or radiative cooling gradients that aid mixing of the contrail with the ambient air.

Contrail Growth and Structure

Once formed, a contrail develops or dissipates in the same manner as a naturally generated cirrus cloud. Growth and spreading of contrails depend on the thickness of the supersaturated layer, the degree of ice supersaturation, and the wind speed and shear. When contrails persist, the particles typically grow to 30–1000 μm, sizes usually associated with natural cirrus clouds. Ice particle growth is rapid in highly supersaturated layers and results in fall streaks that spread horizontally in lower layers according to the wind shear. **Figure 3A** shows a cross-section view of a hypothetical persistent contrail growing and spreading in the absence of vertical wind shear. It spreads mostly by turbulent mixing induced by the aircraft vortex or by radiative processes. When wind shear is present (**Figure 3B**), it will also spread horizontally by precipitation into the lower layers. If the crystals fall

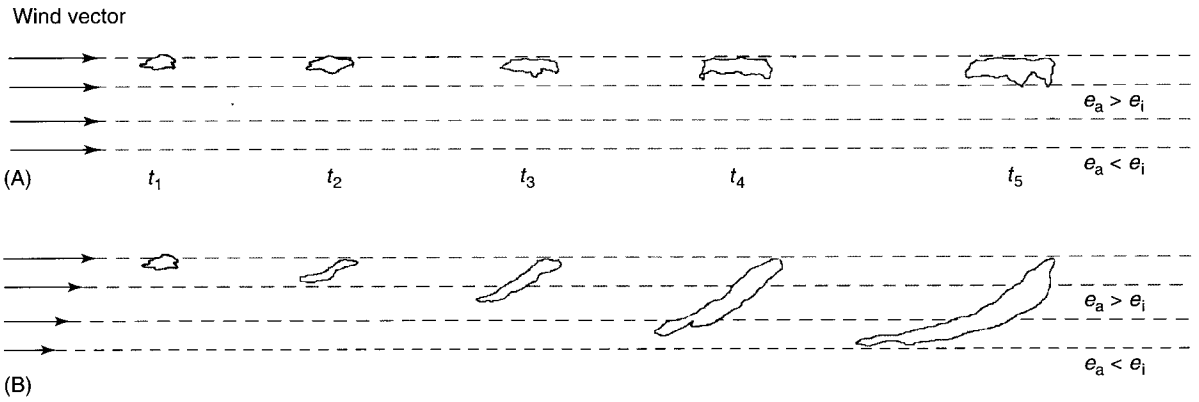

Figure 3 Schematic cross-sectional depiction of contrail spreading in conditions with and without wind shear.

into supersaturated air below, they will continue to grow or, possibly, split into additional crystals. The linear shape of the contrail will be distorted and the contrail will soon look like a natural cirrus cloud to the observer. Well-aged contrails are often indistinguishable from natural cirrus clouds regardless of shear conditions.

Most studies indicate that the number of crystals in a contrail remains constant after formation in supersaturated conditions. Thus, if the contrail precipitates, the contrail cloud at flight level might gradually fade as its particles are depleted. If e_a is just above ice supersaturation, then the crystal growth will be limited and little precipitation will occur. In this case, the contrail may spread slowly by diffusion, maintaining its linear shape for a relatively long time. Because the crystals grow by deposition, the amount of ice water in the contrail increases until the particles fall out or equilibrium is reached between the ice water content and e_i. Such equilibrium conditions generally do not last very long and the contrail eventually dissipates. Although most persistent contrails have visible optical depths between 0.1 and 0.4, the values are highly variable, ranging between 0.03 and 1. The lifetimes of contrails are also extremely variable. Short-lived contrails may only last a few seconds, while some contrail-generated cirrus clouds have been tracked for more than 17 h. The shape, size, optical properties, and life cycle of contrails are highly dependent on their environment, so that a multitude of contrail morphologies can occur. Contrail-cirrus clouds are generally like natural cirrus clouds within a few hours after their formation.

Because water vapor and temperature are not homogeneously distributed, even at relatively small scales (~100 m), contrails may form or persist in an apparently erratic fashion, as shown in **Figure 4**. For example, an on–off pattern can occur as an aircraft flies through a moist layer disturbed by a vertical wave or even weak convective plumes. The contrails in **Figure 4A** form in the ascending parts of the wave or plume where the temperature of the rising air falls below the threshold temperature, while in the descending portions the air warms and dries, resulting in no contrail formation. Similar patterns can result from a plane ascending or descending through several thin layers that are near saturation but separated by dry layers as in **Figure 4B**. The persistence of a contrail or parts of it depends on the value of e_a relative to e_i along the contrail line. Thus, parts of a contrail may dissipate rapidly while other portions may linger and even grow. The local turbulence induced by the airframe, the atmospheric stability, and the wind vector also affect the morphology of the contrail.

Photographs of the most familiar type, the short-lived new contrail, are shown in **Figure 5**. In both cases, the pair of trails forming behind the aircraft gradually faded. In those situations, e_a is only slightly less than e_i. When e_a exceeds e_i, less familiar shapes can occur. **Figure 6** shows examples of contrails at different stages of growth or persistence at the same time in different parts of the sky. To the north of the observer (**Figure 6A**), contrails remain very thin and wispy at one end and dense and distorted at the other. To the south-east (**Figure 6B**), a succession of slowly spreading contrails appears off to the horizon.

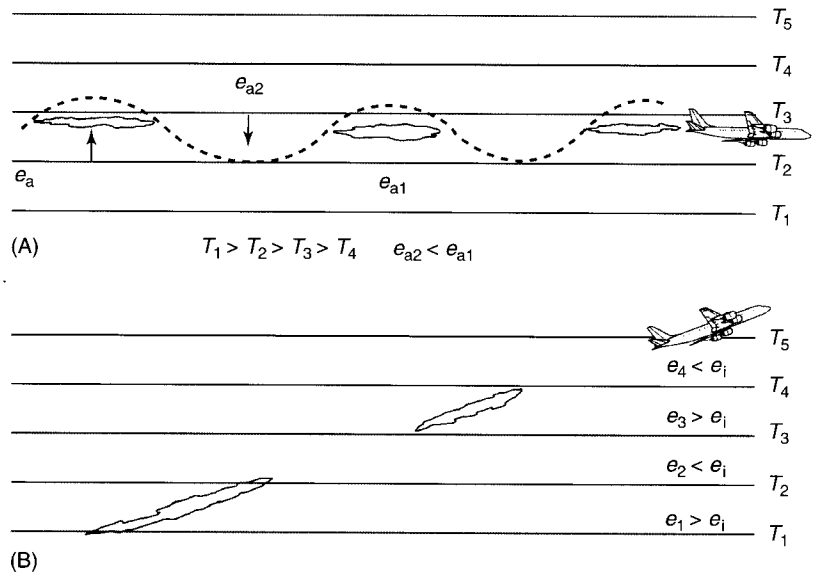

Figure 4 Schematic depiction of contrails forming in an on–off pattern.

Encyclopedia of Atmospheric Sciences, Academic Press, London, J. Holton, J. Pyle, and J. Curry, Editors

Figure 5 Short-lived contrails.

Although these contrails appear to have little vertical development, they persisted for at least several hours before advecting out of view. To the south-west (**Figure 6C**), many of the contrails are older and appear more like natural cirrus clouds. A very young thin contrail is evident in the upper left quadrant.

Condensation trails often form ahead of advancing fronts in the poleward flow of an upper level trough where conditions are not quite saturated enough for natural cirrus development. In these instances they can occur at multiple levels in the atmosphere because the formation conditions often cover a large depth of the atmosphere and air traffic uses a wide range of altitudes. In **Figure 7**, contrails at the higher altitudes spread more than those below owing either to age, the amount of wind shear, or the angle of the contrail to the ambient wind. Note the complex linear shadows cast by the thin contrail on the left. These crossing contrails are common in areas where air traffic lanes intersect. The contrails seen in **Figure 7** are part of a larger contrail cluster that is easily observed in satellite imagery (**Figure 8**) that was taken about an hour before the photograph in **Figure 7**. Subsequent imagery shows that these contrails dissipated downstream to the east while additional contrails formed within or beneath the advancing thin cirrus clouds.

Contrails can form within cirrus clouds, where they are manifest by reduced particle sizes or local thickening of the cloud. Aircraft exhaust can also affect supercooled liquid water clouds. When a plane flies through this type of cloud, it introduces ice nuclei that cause freezing of the cloud droplets. The thermodynamic equilibrium shifts from a vapor-to-liquid to vapor-to-ice process, causing a rapid depletion of the available water vapor onto the frozen droplets. The newly formed ice crystals quickly grow large enough to fall out of the cloud, resulting in a fall streak below the cloud and a gap within the cloud. This gap, called a distrail, is linear when the plane flies for an extended distance within the cloud or oval shaped when the aircraft is briefly inside the cloud as it ascends or

Figure 6 Persistent contrails in various stages of growth and decay.

Encyclopedia of Atmospheric Sciences, Academic Press, London, J. Holton, J. Pyle, and J. Curry, Editors

Figure 7 Persistent contrails observed over eastern Virginia, USA during 26 January 2001. Photo courtesy of L. Nguyen, NASA LaRC.

descends. Depending on the conditions, especially the original cloud thickness, a distrail will either persist or be filled in with a new water droplet cloud. Distrails are most frequently observed in altostratus or altocumulus clouds.

Remote Sensing of Contrails

Although contrails are most often identified by their linear shapes both from ground observations (**Figure 7**) and satellite imagery (**Figure 8**), these

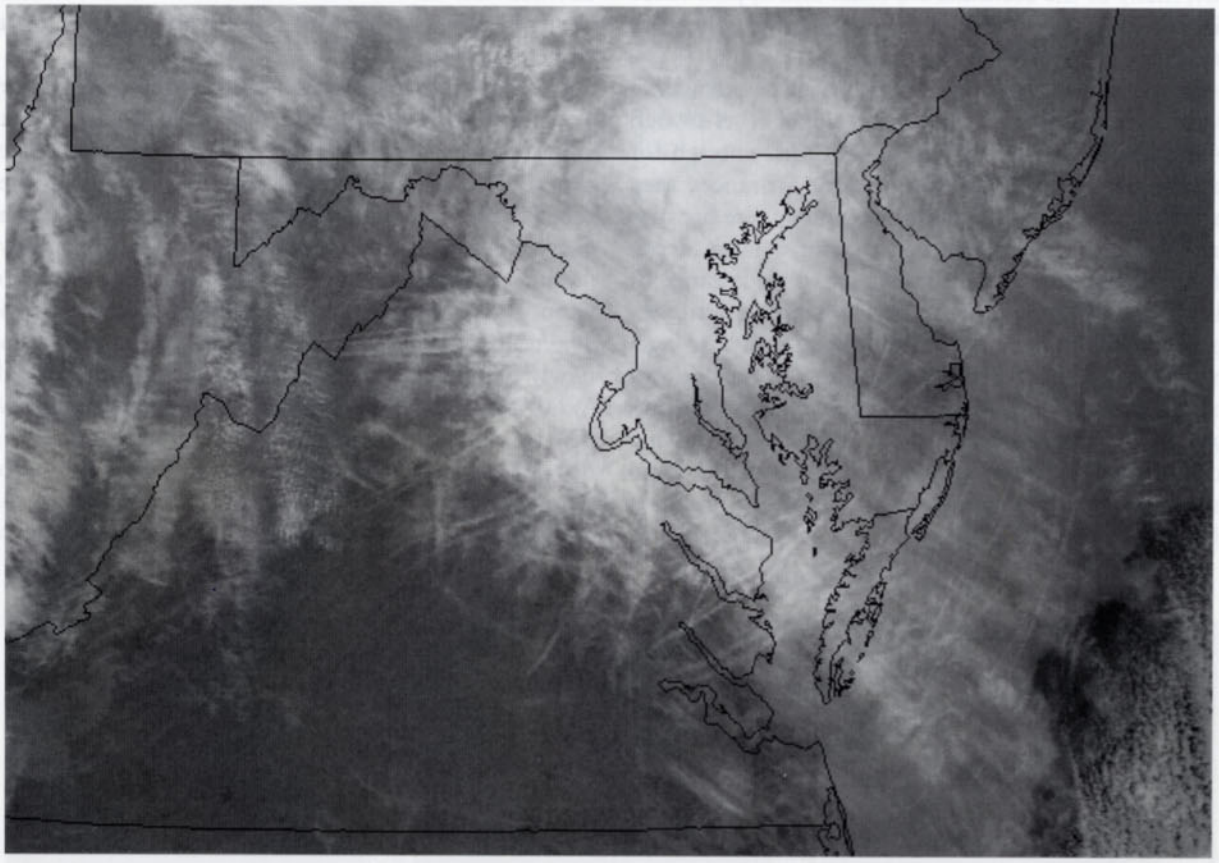

Figure 8 Infrared 1-km resolution image of contrails over Virginia and Maryland, USA from the NOAA-16 Advanced Very High Resolution Radiometer at 1832 UTC, 26 January 2001.

Encyclopedia of Atmospheric Sciences, Academic Press, London, J. Holton, J. Pyle, and J. Curry, Editors

man-made clouds can take on other geometric shapes according to the particular flight patterns and winds. For instance, spiral shapes result from a plane in a circular holding pattern within an advecting supersaturated layer, while a figure-of-eight can form in similar layer if the plane flies a linear holding pattern. The linear structure is most common and forms the basis for identifying contrails. Because detection of contrails is important for various scientific applications, methods have been developed for differentiating contrails from other linear clouds in satellite imagery, the only plausible data source for studying the global effects of contrails. Automated techniques for contrail detection typically create an image of a parameter most likely to be associated with a contrail, then apply a variety of image processing methods to find linear structures within that image.

Such methods, which are still being researched, usually take advantage of the relatively distinct infrared optical properties of younger contrails to compute a parameter that could have a distinctive contrail signal for image processing. Because of their relatively small size (effective diameters between 5 and 50 μm), the ice crystals in contrails have extinction efficiencies in the thermal infrared window region (8–14 μm) that vary much more with wavelength than the extinction efficiencies of larger particles typically found in most cirrus clouds (effective diameters greater than 30 μm). Thus, young contrails transmit more radiation at certain wavelengths than a cirrus cloud of equivalent optical depth, resulting in a signal that often reveals a contrail.

To better understand this effect, consider that the satellite measures a spectral radiance L_λ that is recorded as an equivalent blackbody temperature T_λ using the Planck function B_λ. For a cloud or contrail, the observed radiance can be modeled simply as in eqn [4].

$$L_\lambda = \varepsilon_\lambda L_c + (1 - \varepsilon_\lambda) L_b \qquad [4]$$

where L_c is the radiance emitted at the cloud temperature T_c, L_b is the upwelling radiance at the cloud base with an equivalent brightness temperature T_b, and ε_λ is the cloud emissivity. In general, $L_b > L_c$, so that an increase in cloud transmissivity, $(1 - \varepsilon_\lambda)$, results in more transmission of L_b and a larger value of L_λ. Thus, T_λ will be greater at some wavelengths than at others as long as the cloud is optically thin (ε less than 0.9 or so). This effect can be seen in **Figure 9**, which shows the 11 μm image and an image of brightness temperature difference between the 11 μm and 12 μm channels on the NOAA-12 Advanced Very High Resolution Radiometer. For small ice crystals, the extinction efficiency and, therefore, the optical depth at 12 μm can be as much as twice that at 11 μm. Thus, for small optical depths (<1.0), the transmission at 11 μm is greater and the contrails appear 'warmer' than at 12 μm. Although some of the contrails are readily apparent in **Figure 9A**, many are obscured by other cirrus clouds. The temperature-difference image in **Figure 9B** reveals many contrails that were not evident in the standard infrared image and highlights others more clearly. Because the actual temperature difference contrast depends on the effective particle sizes and optical depths of the surrounding clouds, and those quantities are naturally variable, the contrails are not always detected. Furthermore, other features such as cirrus streaks, coastlines, or cloud edges may produce similar signals.

When T_b is not very different from T_c, such techniques do not readily reveal the contrails because

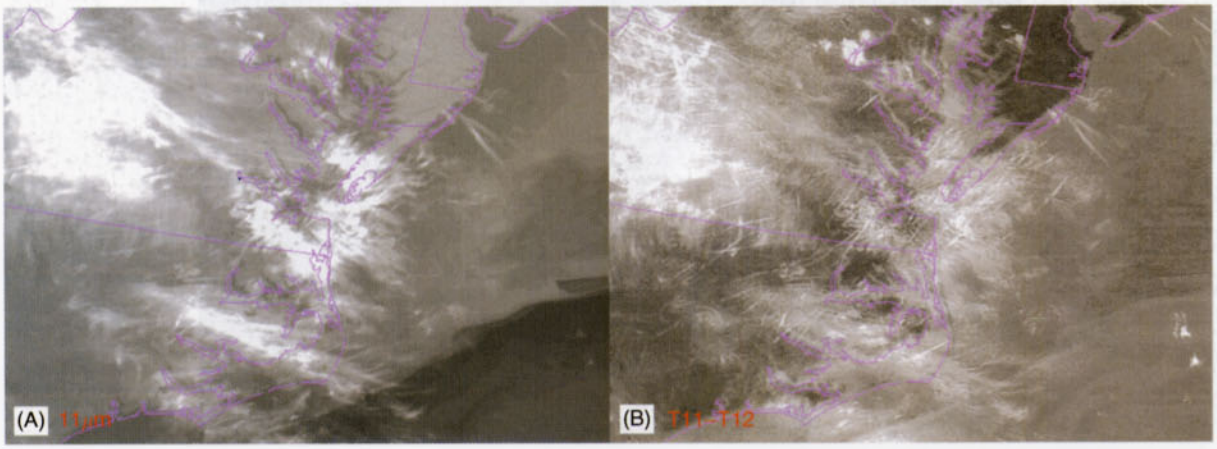

Figure 9 1-km resolution infrared and infrared temperature difference images of contrails over Virginia and North Carolina, USA from the NOAA-12 Advanced Very High Resolution Radiometer at 2312 UTC, 29 October 1996.

the signal is so small. Therefore, contrails embedded in relatively thick cirrus clouds cannot be seen in most temperature-difference imagery. However, during the daytime, contrails can be detected using temperature differences between a channel near 11 μm and one in the 'solar-infrared' wavelength range (3.5–4.5 μm). At those wavelengths, the satellite imagers measure an emission component and a solar-reflected component. The smaller contrail ice crystals reflect more sunlight than the surrounding cirrus crystals, resulting in a relatively large brightness temperature. For example, the 11 μm image in **Figure 10** shows no sign of contrails, while the 3.7 μm image and the 11 μm and 3.7 μm temperature-difference image reveal a number of linear contrails. The 3.7 μm image shows dark or 'warm' lines, while the temperature-difference image reveals white contrails. Additional enhancement of the photograph would reveal more contrails in the temperature-difference image. The ability to detect contrails in a thick cirrus cloud depends on many factors, including the contrail age and its relative depth in the cloud as well as the particle sizes in

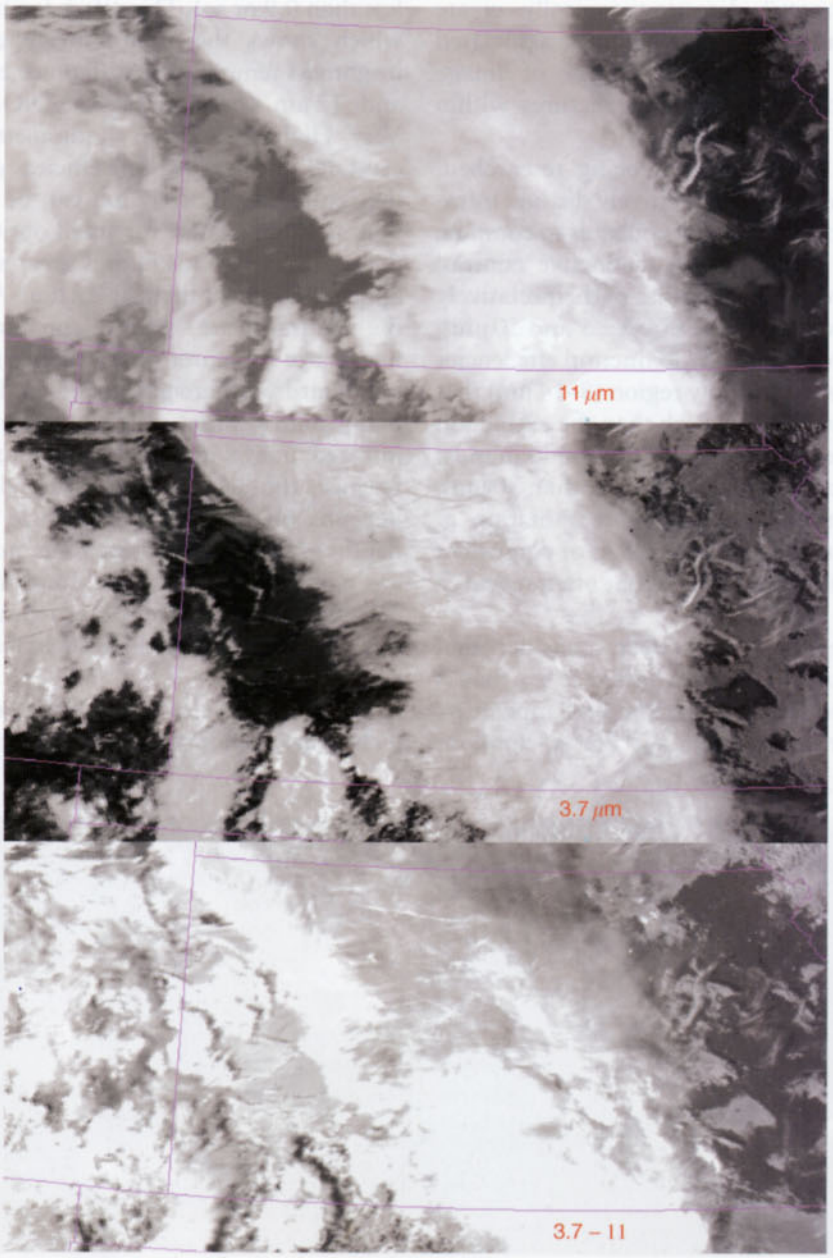

Figure 10 Contrails imbedded in thick cirrus over Kansas, USA from NOAA-14 Advanced Very High Resolution Radiometer data taken at 2122 UTC, 23 March 2000.

the cirrus cloud, and the viewing and illumination conditions.

Contrails can also be detected in high-resolution visible and near-infrared imagery in certain conditions. For example, when not embedded in cirrus or over lower clouds, a young contrail is often reflective enough to be seen as a bright line in a 1-km resolution visible channel image. Sometimes, the contrail will cast a shadow on lower clouds and can be detected from its shadow. Near-infrared channels on or near water vapor absorption lines, like one near 1.38 μm, do not receive any significant reflectance from lower clouds, so that even very thin high clouds like contrails can be detected. Near-infrared methods are relatively new and have not been developed as much as the infrared techniques.

Determination of contrail properties such as temperature, height, optical depth, and effective particle size is accomplished with the same methods applied to the remote sensing of cloud properties. Such techniques typically require multispectral imagers that can be used to simultaneously solve for ε, T_c, and the particle size. When an insufficient multispectral set is available, one or more of the parameters must be assumed in order to obtain a solution for the other parameters. These methods generally provide results consistent with *in situ* measurements. Both infrared and solar methods are also applicable to high-resolution imagery created by instruments on research aircraft. Active sensors such as lidar have been used to study the fine-scale structures of contrails and their microphysical properties. They are often used to validate the retrievals of contrails from passive satellite imagers.

Contrail–Cirrus Coverage

An increase in cirrus cloudiness due to contrail formation has been hypothesized since the beginning of the commercial jet age. The possibility of enhanced cirrus coverage resides in the frequency and extent of areas that are ice-supersaturated. *In situ* measurements and numerical model analyses have shown that e_a exceeds e_i 10–20% of the time in air at flight altitudes (8–12 km). Thus, the potential exists for substantial increases in cirrus coverage over areas crossed by air traffic. Because the stratosphere is generally very dry, aircraft flying above the tropopause generate few contrails, especially persistent ones.

The conditions necessary for supporting contrail formation at flight altitudes change with the seasons. Over mid-latitude areas, contrail conditions are favorable most often during winter and early spring when the troposphere is coldest. During summer, the temperatures at flight levels are often too high to enable contrail initiation. Over areas poleward of about 50° latitude, the tropopause is often below flight level during winter, so that a significant number of planes fly in the stratosphere, resulting in contrail suppression. Conditions are more favorable for contrails during the summer and autumn in the subarctic regions. In the tropics, the altitude for contrails is generally above 11 km year round, so the potential for contrail formation by many commercial planes is reduced. However, persistent contrails are likely to occur more frequently in the tropics than at other latitudes at altitudes above 11 km because of the greater abundance of water vapor.

Surface observations over the United States during the 1990s indicated that persistent contrails occur, on average, approximately 9% of the time, but the frequency varies from less than 5% in low traffic areas to 25% in the main air corridors. Approximately 80% of these persistent contrails are embedded in, extending from, or near natural cirrus clouds. Contrail coverage has been derived from satellite imagery only for those contrails that are linear and large enough to observe in 1-km resolution infrared data. Initial satellite-based estimates of mean contrail amounts over Europe, the North Atlantic, and the conterminous United States are 0.8%, 0.5%, and 1.8%, respectively, and roughly 0.1% globally for the early 1990s. Similar values have been derived from theoretical calculations using realistic air traffic patterns, numerical analyses of meteorological fields, and specified engine efficiencies. Later studies suggest that the coverage may not be as large as the initial satellite estimates owing to possible false identification of natural clouds as contrails.

Detection and assessment of contrail coverage has been confined to contrails that are identifiable by their linear structure and small particle sizes. Because these identifying features are often lost as the contrails spread, the linear contrail coverage estimates represent the minimum amount of the sky that is covered by contrails. Geostationary satellite data are used to track contrails as they grow and change in shape and composition. Studies based on geostationary data indicate that the actual cirrus coverage generated by persistent contrails might be as large as a factor of 4 times the coverage estimated for younger, linear contrails. However, the actual factor is probably somewhere between 1 and 3. Determination of contrail coverage and the resulting changes in cirrus cloud amounts remains a topic of ongoing research.

Climate Effects of Contrails

Contrails, like other cirrus clouds, can affect both the hydrological and radiation budgets. Many of the possible contrail effects have only been the subject of educated speculation, although some have been estimated to some degree. Some of these potential effects are mentioned here.

By freezing out water vapor prior to the natural formation of cirrus clouds, contrails may alter the overall distribution of cirrus. General circulation model studies have shown that, if additional cirrus cloud is specified in the air corridors, cirrus coverage decreases in other areas. Contrail formation may decrease precipitation in some clouds by reducing the average particle size in the affected clouds. Conversely, the precipitation induced by persistent contrails in otherwise clear air (e.g., **Figure 3A**) may result in moistening of the middle layers of the troposphere and drying of the atmosphere at flight altitudes.

Contrails reflect some solar or short-wave radiation that would otherwise warm the surface, and absorb outgoing infrared radiation that cools the surface–atmosphere system. The overall radiative impact or forcing depends on the contrast between the contrail and its background, the lifetime and optical properties of the contrail, and the solar zenith angle when it is present. Depending on the solar zenith angle and the contrast between the contrail and surface temperatures, the net forcing can result in cooling or warming of the system. For instance, if the contrail forms over a dark background during midday, the amount of reflected sunlight may exceed the amount of infrared radiation blocked and reradiated by the cloud. Conversely, if it develops over a bright, hot surface (i.e., desert) during the day, a contrail may reflect little additional radiation, but trap a significant amount because it is much colder than the surface. Its overall impact would be substantially different than that over the dark surface. At night, contrails warm the atmosphere. However, even during the day when solar and infrared forcing can almost cancel each other, the contrail will still impact the radiation field because loss of most of the blocked sunlight results in cooling of the surface, while much of the infrared or longwave radiation 'trapped' by the contrail warms the upper troposphere and has little immediate impact on the surface.

These radiative forcing effects, estimated with several different models and assumptions, may result in a minor amount of global warming when averaged over a long period or in some slight cooling on an instantaneous basis. For example, **Figure 11** shows the distribution of net contrail radiative forcing assuming random contrail/cloud overlap, an average contrail particle effective diameter of 24 μm, and an optical depth of 0.1. This estimate, based on air traffic analyses for 1992, shows the areas of strongest warming over the north-eastern United States and Europe. The maximum forcing of 0.35 W m^{-2} is found over Europe, while the overall global net forcing for

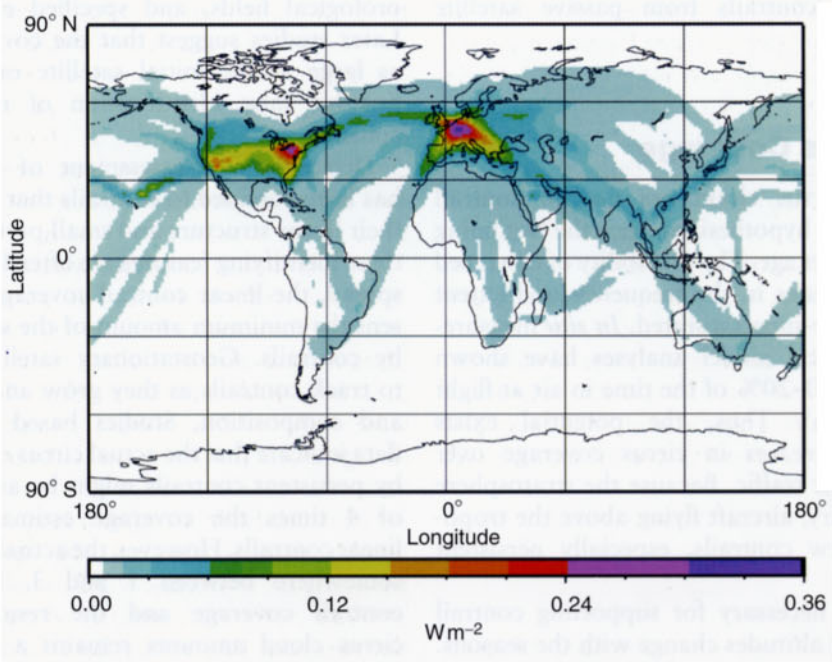

Figure 11 Estimate of radiative forcing from linear contrails with a mean optical depth of 0.1 at 200 hPa for 1992.

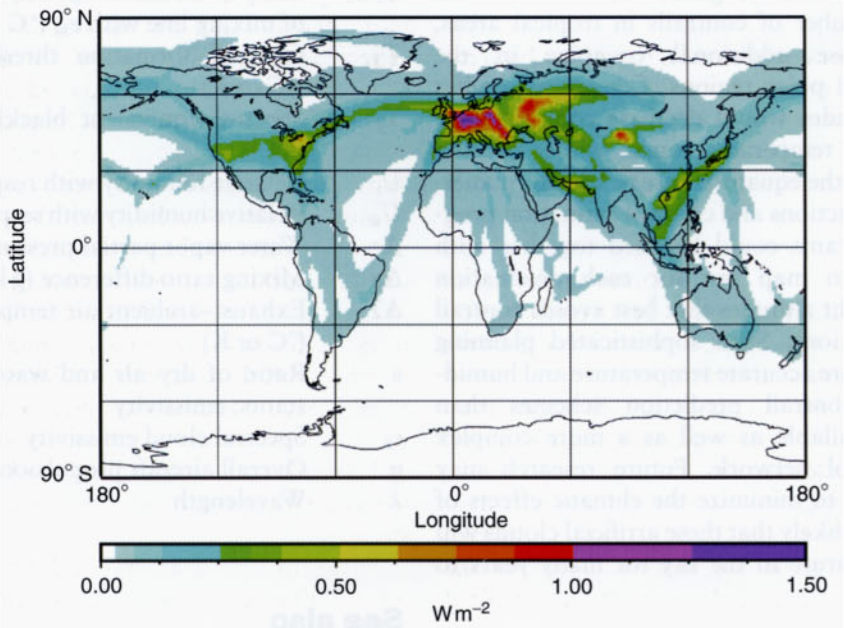

Figure 12 Estimate of radiative forcing from linear contrails with a mean optical depth of 0.1 at 200 hPa for 2050 air traffic scenario.

this case is 0.0083 W m^{-2}. Other scenarios yield values between 0.0004 and 0.0203 W m^{-2} for a range of contrail coverage and altitudes with mean optical depths varying between 0.1 and 0.5 (**Figure 12**). Airplane fuel consumption is expected to increase between 1992 and 2050 by a factor ranging from 1.8 to 14. The best-case scenario yields a factor of 4.3 for traffic above 500 hPa with a concomitant rise in efficiency to $\eta = 0.5$. The greatest increases in air traffic are expected over eastern Europe and Asia. The combination of engine efficiency and air traffic increase yields an estimate of global contrail coverage of 0.5% and a 0.0488 W m^{-2} global net radiative forcing, with a maximum regional value of 1.46 W m^{-2} over Europe. Other scenarios using different contrail radiative properties and fuel use projections produce both smaller and larger estimates of contrail cover and radiative forcing for the future. Current uncertainties in contrail coverage, optical depth, lifetimes, and overlap with lower clouds preclude a definitive assessment of the overall impact of contrails. Despite these uncertainties, it is clear that whatever effect they currently have on climate will increase in the future.

The Future

Contrails are difficult to study because of their high altitude, large advection rates, and frequent association with natural cirrus. Thus, current estimates of their impact are highly uncertain. Nevertheless, their potential for affecting global climate and providing military intelligence has spurred more interest and focused research into their formation, dissipation, microphysical and morphological characteristics, and methods for suppressing them. Removal of fuel sulfur or use of liquid hydrogen fuels have been suggested as means for diminishing the number of cloud nuclei and, hence, the number of contrails. Tests and theoretical studies have shown that such measures would probably not reduce the frequency of contrails. Hydrogen fuels would cause larger increases in local relative humidity in the exhaust plume, causing higher supersaturations than would occur with hydrocarbon fuels. Thus, liquid hydrogen would probably cause more contrails to form, but possibly with greater particle sizes and fallout rates, resulting in shorter lifetimes and smaller radiative impacts. It is possible that a propulsion source that does not produce water vapor will be necessary to effectively eliminate the generation of contrails from high-flying aircraft.

Other methods for minimizing contrail formation would involve changes in flight altitude or path. Contrail coverage could be reduced dramatically by flying in the stratosphere, where formation conditions are rare. However, other effects from the exhaust and increased fuel usage may limit the amount

of stratospheric traffic. Flying at lower altitudes would diminish the number of contrails in tropical areas, but would cause additional coverage in the mid-latitudes and polar regions. Conversely, higher mean flight altitudes would decrease contrails over the poles and temperate zones while causing more contrails in the equatorial areas. Ideally, numerical weather predictions and contrail formation prognostication programs could be used together with flight planners to map out for each destination a sequence of flight altitudes that best avoids contrail formation conditions. Such sophisticated planning would require more accurate temperature and humidity data and contrail prediction schemes than are currently available as well as a more complex air traffic control network. Future research may provide the tools to minimize the climatic effects of contrails, but it is likely that these artificial clouds will be a common feature in the sky for many years to come.

Nomenclature

B_λ	Planck function
c_p	Specific heat capacity ($J\,kg^{-1}\,K^{-1}$)
e_a	Ambient water vapor partial pressure (Pa)
e_e	Exhaust water vapor partial pressure (Pa)
e_i	Ice saturation partial pressure (Pa)
e_w	Liquid water saturation partial pressure (Pa)
EI_w	Water vapor emission index ($kg\,kg^{-1}$)
G	Exhaust–ambient air mixing line slope ($Pa\,K^{-1}$)
h_p	Specific plume enthalpy ($J\,kg^{-1}$)
p	Pressure (hPa)
q	Water vapor mixing ratio ($g\,kg^{-1}$)
L_b	Upwelling radiance at cloud base ($W\,m^{-2}\,sr^{-1}$)
L_c	Radiance emitted by cloud ($W\,m^{-2}\,sr^{-1}$)
L_λ	Spectral radiance ($W\,m^{-2}\,sr^{-1}$)
Q	Mass specific combustion heat ($MJ\,kg^{-1}$)
t	Time (s)
T	Temperature (°C or K)
T_a	Ambient temperature (°C or K)
T_b	Equivalent blackbody temperature of upwelling radiance at cloud base (K)
T_c	Cloud temperature (K)
T_e	Exhaust temperature (°C or K)
T_F	Temperature corresponding to tangent point of mixing line with e_w (°C or K)
T_T	Contrail formation threshold temperature (°C or K)
T_λ	Spectral equivalent blackbody temperature (K)
U_i	Relative humidity with respect to ice
U_w	Relative humidity with respect to liquid water
Δe	Water vapor partial pressure difference (Pa)
Δq	Mixing ratio difference ($g\,kg^{-1}$)
ΔT	Exhaust–ambient air temperature difference (°C or K)
ε	Ratio of dry air and water vapor gas constants; emissivity
ε_λ	Spectral cloud emissivity
η	Overall aircraft propulsion efficiency
λ	Wavelength

See also

Aerosols: Role in Cloud Physics. **Aircraft Emissions**. **Cloud Microphysics**. **Clouds:** Classification. **Convection:** Laboratory Models of. **Global Change:** Human Impact of Climate Change. **Optics, Atmospheric:** Optical Phenomena; Optical Remote Sensing Instruments. **Radiative Transfer:** Cloud-radiative Processes. **Satellite Remote Sensing:** Cloud Properties. **Thermodynamics:** Saturated Adiabatic Processes.

Further Reading

Brasseur GP, Hauglustaine D, Cox RA, *et al.* (1998) European scientific assessment of the atmospheric effects of aircraft emissions. *Atmospheric Environment* 32 (13): 2329–2418.

Penner JE, *et al.* (1999) *Aviation and the Global Atmosphere*. Cambridge: Cambridge University Press.

Schumann U (1996) On conditions for contrail formation from aircraft exhausts. *Meteorologische Zeitschrift* 5: 4–23.

Schumann U and Amanatidis GT (2001) Aviation, aerosols, contrails, and cirrus clouds (A^2C^3). *Air Pollution Research Report* 74. European Commission, Brussels, Belgium.

Toon OB, *et al.* (1996) Subsonic aircraft: contrail and cloud effects special study. *Geophysical Research Letters* 25(8): 1109–1168.